AppliedChem

Article

Comparative Study of Various Graphene Oxide Structures as Efficient Drug Release Systems for Ibuprofen

Panagiota Zygouri [1,2,*], Konstantinos Spyrou [1,2], Demetrios K. Papayannis [1], Georgios Asimakopoulos [1], Evangelia Dounousi [3], Haralambos Stamatis [4], Dimitrios Gournis [1] and Petra Rudolf [2,*]

[1] Department of Materials Science and Engineering, University of Ioannina, GR-45110 Ioannina, Greece; konstantinos.spyrou1@gmail.com (K.S.); dpapagia@uoi.gr (D.K.P.); asimakopoulos.geo@gmail.com (G.A.); dgourni@uoi.gr (D.G.)
[2] Zernike Institute for Advanced Materials, University of Groningen, Nijenborgh 4, 9747 AG Groningen, The Netherlands
[3] Department of Nephrology, Medical School, University of Ioannina, GR-45110 Ioannina, Greece; edounous@uoi.gr
[4] Department of Biological Applications and Technology, University of Ioannina, GR-45110 Ioannina, Greece; hstamati@uoi.gr
* Correspondence: pzygouri@gmail.com (P.Z.); p.rudolf@rug.nl (P.R.); Tel.: +30-265-100-7351 (P.Z.); +31-503-634-736 (P.R.)

Abstract: Ibuprofen is a non-steroidal, anti-inflammatory drug that is widely prescribed for its analgesic, antipyretic, and anti-inflammatory actions to treat pain, symptoms of rheumatoid arthritis and fever, but it is also known to cause stomach-related side effects. The development of efficient drug delivery systems for this compound to prevent these side effects is hampered by its poor water solubility. In this work, we show that graphite oxide and its derivatives have great potential as effective drug delivery systems not only to overcome side effects but also to increase the short biological half-life of ibuprofen. We studied the adsorption capacity of graphite oxide and carboxylated and sulfonated graphene oxide for this drug and its release in simulated gastric and intestinal fluid. The obtained compounds were characterized by X-ray diffraction, thermogravimetric analysis and Fourier transform infrared spectroscopy. DFT calculations were conducted to elucidate the Ibuprofen/host interactions, to establish which properties of these carbon nanomaterials control the loading and release, as well as to provide a better understanding of the orientation of the drug molecules on the single-layer GO.

Keywords: graphene oxide; ibuprofen; release study; theoretical calculations; intercalation

Citation: Zygouri, P.; Spyrou, K.; Papayannis, D.K.; Asimakopoulos, G.; Dounousi, E.; Stamatis, H.; Gournis, D.; Rudolf, P. Comparative Study of Various Graphene Oxide Structures as Efficient Drug Release Systems for Ibuprofen. *AppliedChem* **2022**, 2, 93–105. https://doi.org/10.3390/appliedchem2020006

Academic Editor: Jason Love

Received: 14 April 2022
Accepted: 30 May 2022
Published: 6 June 2022

1. Introduction

The efficacy of a drug delivered orally to the gastrointestinal tract depends on multiple factors that restrict its performance. Such drawbacks can be the lack of bioavailability of the drug, which may derive from low solubility or dissolution rate [1]. Almost 40% of new drugs released face severe problems due to poor solubility and bioavailability [1,2], leading to ineffective therapies or undesirable side effects caused by increasing the drug dose to overcome these issues. Ibuprofen is a non-steroidal anti-inflammatory drug (NSAID) that is also an antipyretic analgesic. In many cases, its use is limited by the very common undesirable gastrointestinal side effects (>1/10 patients). Ibuprofen belongs to the category of hydrophobic drugs, and consequently, enhancing its solubility is of great importance. A solution to overcome these obstacles is to employ nanometer-sized delivery systems, able to carry the drug in high concentrations so as to retain the delivery profile while avoiding solubility and toxicity problems.

A plethora of drug delivery systems have been proposed to ensure a controlled release rate and targeted delivery [3]; in fact, proteins, lipids, polymers, and organic and

inorganic materials have been investigated for this purpose [4,5]. Among them, carbon-based materials are an important class of drug carriers. Elemental carbon possesses multiple allotropic forms and arrangements depending on the type of hybridization (sp^3, sp^2, sp). This leads to structures with specific dimensions and shapes such as graphite, carbon nanotubes, nanodiamonds, fullerenes, graphene, and many others, which, in combination with excellent physicochemical properties [6], good biocompatibility [7] and an easily accessible and functional surface area [8], occupy a distinctive position as nanomedical scaffolds compared to other drug delivery systems.

Graphite oxide (GO) is ideal as a drug carrier [9–12] because it is decorated with various oxygen-containing moieties that assure solubility and can be exploited for functionalization. It possesses a two-dimensional planar structure with a delocalized π electrons system, is chemical stable, has a large surface area (500 m^2/g) [13] and can interact with plenty of biomolecules [14,15]. Graphite oxide can accommodate aromatic drugs such as ibuprofen through hydrophobic and π–π interactions [16]. GO and its derivatives with various surface groups for interaction with proteins, genes, drugs, DNA, and antibodies have been shown to have great potential for diagnostics and treatment processes [17–19] related, e.g., to cancer therapy [20,21], antitumor activity [22,23], and gene delivery [24,25].

The aim of this work was, therefore, to find out if controlling the release of ibuprofen (IBU) (Figure 1) while overcoming its side effects and increasing its short half-life (1.8–2.0 h) can be added to the potential applications for these carbon structures. More specifically, the intercalation of ibuprofen into graphite oxide (GO), sulfonated graphite oxide (GO_OSO_3H) and carboxylated graphite oxide (GO_COOH) was studied, and the efficacy of these nanomaterials as delivery systems for ibuprofen was determined. The amount of ibuprofen absorbed in each case was determined from UV–Vis measurements, and the release of the drug in simulated gastric and intestinal fluids was investigated.

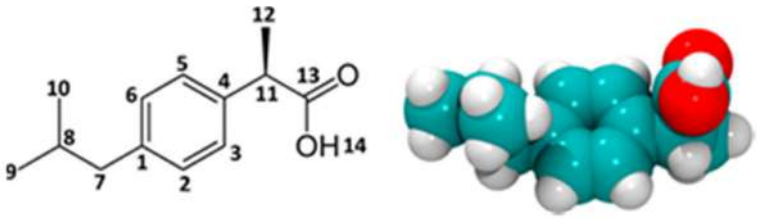

Figure 1. Structure of 2-(4-isobutylphenyl)-propionic acid ($H_{18}C_{13}O_2$) or ibuprofen: (**left**) 2D chemical structure with atom numbering; (**right**) 3D space-filling model of the B3LYP-optimized, most stable conformer.

Knowing the superior properties of graphene and graphene oxide as ideal systems for a broad range of biomedical applications (including drug delivery nanocarriers), in this work we wanted to focus on the abilities of graphene to improve its therapeutic profile as an efficient drug carrier by applying carbon chemistry. Three different graphene-based nanomaterials with different functional groups on their surfaces were effectively synthesized to study their behavior on the adsorption of ibuprofen. This study will pave the way for future biomedical studies on different carbon-based materials.

2. Materials and Methods

2.1. Preparations of Materials

2.1.1. Preparation of Graphite Oxide (GO)

The oxidation of graphite was performed by adding 5 g of powdered graphite (purum, powder $\leq$ 0.2 mm, Fluka) to a mixture of concentrated sulfuric acid and nitric acid (200 mL, 95–97 wt.% and 100 mL, 65 wt.%, respectively) while cooling in an ice-water bath for 20 min. Thereafter, 100 g of powdered $KClO_3$ (Fluka) were added to the mixture in small portions under vigorous stirring. The reaction was completed after 18 h by pouring the mixture

into ultrapure water, and the product was washed until the pH reached 6.0. Finally, the obtained sample was dried at room temperature [26].

2.1.2. Preparation of Sulfonated Graphite Oxide (GO_OSO_3H)

In a spherical flask, 6 g of graphite oxide and 300 mL sulfuric acid with concentration of 95–97% were combined, and the mixture was stirred for 3 days under nitrogen atmosphere. Thereafter, the mixture was placed in an ice bath and 600 mL of anhydrous diethyl ether were added in small portions under vigorous stirring. The sample was centrifuged and washed twice with diethyl ether before being dried in vacuum at 40 °C overnight [27].

2.1.3. Preparation of Carboxylated Graphite Oxide (GO_COOH)

Five hundred milligrams of graphite oxide were dispersed in 250 mL of distilled water by stirring. Twenty-five grams of $ClCH_2COOH$ and 30 mL of NaOH (1M) were then added, and the mixture was sonicated for 3 h. After that time, an aqueous HCl solution (1M) was added in small portions until the pH value reached 7. The resulting mixture was centrifuged and washed with distilled water before being dried at room temperature [28].

2.1.4. Intercalation of Ibuprofen into Graphite Oxide (GO), Sulfonated Graphite Oxide (GO_OSO_3H) and Carboxylated Graphite Oxide (GO_COOH)

In the effort to study graphite oxide as an efficient drug delivery system for ibuprofen, 180 mg of IBU was dispersed in 10 mL of EtOH (absolute) and 300 mg of GO in 30 mL of distilled water. The two dispersions were mixed, and the mixture stirred for 24 h while heating at 50 °C. The solid part was separated by centrifugation (4000 rpm, 30 min), and the supernatant was filtered through a Millipore filter (0.45 μm FG). The resulting sample was denoted by IBU/GO. The above synthetic procedure was also followed for sulfonated and carboxylated graphite oxide [29]; the resulting samples were denoted by IBU/GO_OSO_3H and IBU/GO_COOH. In each case, the IBU concentration in the supernatant was determined via UV–Vis spectroscopy at λ = 222 nm after dilution, while the intensity of the same absorption peak was determined for pure ibuprofen as a reference.

2.2. In Vitro Drug Release of Ibuprofen

One hundred milligrams of either IBU/GO or IBU/GO_OSO_3H or IBU/GO_COOH and 50 mL simulated gastric fluid were added into dialysis membrane bags. The membrane bags were sunk in 200 mL gastric fluid (Sigma-Aldrich, St. Louis, MO, USA), and the beakers were placed in an isothermal shaker bath at 37 °C, where they were continuously shaken for 24 h. Three milliliters of the dissolution media were sampled for the UV–Vis measurements to determine the percentages of the released Ibuprofen as explained above. Immediately after taking these samples, the dissolution media were refilled in order to keep the volume constant. Measurements were taken every 30 min. The procedure was repeated with simulated intestinal fluid (Sigma-Aldrich) in place of the gastric fluid to monitor the drug release from these nanomaterials in that medium.

2.3. Characterization Techniques

The XRD patterns were collected on a D8 Advance Bruker diffractometer by using Cu Kα radiation (40 kV, 40 mA) and a secondary beam graphite monochromator. The patterns were recorded in the 2-theta (2Θ) range from 2 to 80°, in steps of 0.02° and a counting time of 2 s per step. Samples were in the form of films supported on glass substrates. For the preparation of the films, aqueous suspensions of the hybrids were deposited on glass plates and the solvent was allowed to evaporate slowly at ambient temperature. Infrared spectra in the region of 400–4000 cm^{-1} were measured with a PerkinElmer Spectrum GX infrared spectrometer, equipped with a deuterated triglycine sulphate (DTGS) detector. Each spectrum was the average of 64 scans collected with 2 cm^{-1} resolution. Samples were in the form of KBr pellets containing ca. 2 wt.% sample. Thermogravimetric (TGA) and differential thermal (DTA) analyses were performed using a PerkinElmer Pyris Diamond

TG/DTA. Samples of approximately 5 mg were heated in air from 25 °C to 850 °C, at a rate of 5 °C/min. UV–Vis spectra were collected on a Shimadzu UV-2401PC two-beam spectrophotometer in the range of 200–800 nm, with steps of 0.5 nm, using a combination of deuterium and halogen lamps as sources. Atomic force microscopy (AFM) images were recorded in tapping mode with a Bruker Multimode 3D Nanoscope, using Tap-300G silicon cantilevers with a tip radius of <10 nm and a force constant of ≈20–75 N m^{-1}. Samples were deposited onto silicon wafers (P/Bor, single side polished, purchased from Si-Mat) from water dispersions by drop casting.

2.4. Computational Methods

DFT calculations were performed adopting the Becke, 3 parameters, Lee−Yang−Parr (B3LYP) hybrid functional [30,31]. B3LYP is still recognized as one of the most widely used and well-balanced functionals since its accuracy is warranted by the enormous database of results accumulated over the years. All calculations were carried out by means of the Gaussian 09 Quantum Chemistry Package [32], and the stable geometries were calculated with a tight criterion geometry optimization. For all calculations and all involved atoms, the standard 3-21G* double-ζ valence basis set [33] with more accurate results on large systems was used and implemented in the selected geometrical models. The geometry optimizations were carried out without imposing any symmetry restrictions and followed by an estimation of vibration fundamentals via harmonic frequency calculations.

Specifically, the graphite surface was modeled by means of a $C_{80}H_{22}$ cluster that represents a nanometer-size graphite crystallite (Figure 2). This cluster was used to study the interaction of the ibuprofen molecule with the single-layer GO. The graphene nanosheet was represented in the modeling studies by 30 fused benzene rings arranged in a single atomic layer containing 80 carbon atoms, with the edges saturated by hydrogen atoms, corresponding to the molecular formula $C_{80}H_{22}$. It was then treated quantum mechanically as a single-layer hydroxylated graphene oxide model cluster ($C_{80}H_{30}O_{18}$) GO, a single-layer carboxylated graphene oxide model cluster ($C_{80}H_{30}O_{16}$) GO_COOH, and a single-layer sulfonated graphene oxide model cluster ($C_{80}H_{30}O_{32}S_8$) GO_OSO_3H, calculated at the B3LYP/3-21G* level of theory. The vibrational modes and the corresponding frequencies for the GO cluster models with ibuprofen and ibuprofen anion were based on a harmonic approximation (HO), which was accomplished for all calculated structures using the same level of theory.

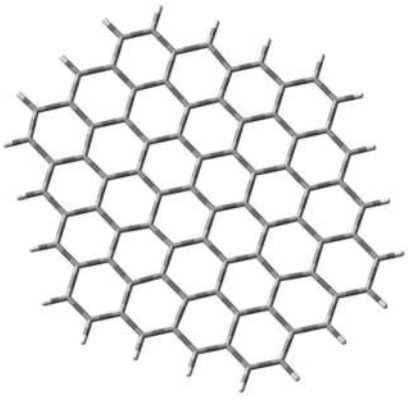

Figure 2. Graphene cluster ($C_{80}H_{22}$) consisting of 30 rings and saturated with hydrogen atoms (top view).

After the optimization of the cluster models, ibuprofen was added to the system and allowed to assume an optimized position by varying the distance between IBU and the GO models. During structure optimization, only the adsorbed IBU molecule, the terminal hydrogens of the graphene nanosheet and the –O–, –OH, –COOH and –OSO_3H groups, decorating the surface and the edges of the graphene layers with the corresponding linking

carbon atoms, were allowed to relax, while the remaining atoms in the atomic layer were kept fixed at the crystallographic positions.

3. Results

3.1. Material Characterization

Figure 3 displays the FTIR spectra of IBU/GO, IBU/GO_COOH and IBU/GO_OSO_3H together with those of pure IBU and of the host matrices. The characteristic absorption bands of IBU appear in the spectrum of each loaded matrix, which confirms the successful inclusion of IBU in all three nanomaterials. More specifically, the band at 1721 cm^{-1} is attributed to stretching vibrations of carbonyl groups (C=O), and the bands observed in the range of 2800–3000 cm^{-1} are related to the stretching vibration of alkyl groups of IBU. The band at 1512 cm^{-1} corresponds to C-C vibrations, whereas the band at 1452 cm^{-1} is due to the asymmetric bending vibration of C-H (CH_3) and the scissoring vibration of C-H (CH_2). In the region 1100–1300 cm^{-1}, the 3 bands at 1268 cm^{-1}, 1230 cm^{-1} and 1184 cm^{-1} are attributed to stretching vibrations of C-O and bending vibrations of O-H [29,34].

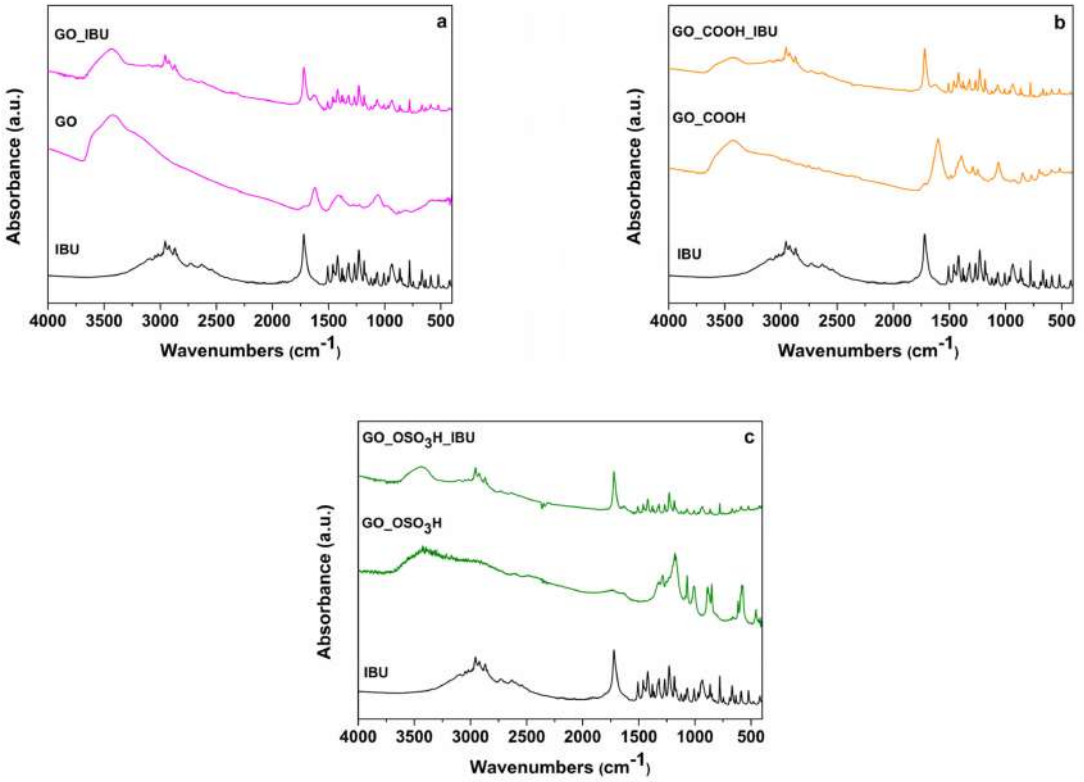

Figure 3. FTIR spectra of (**a**) ibuprofen (IBU), graphite oxide (GO) and the ibuprofen/graphite oxide composite (IBU/GO); (**b**) ibuprofen (IBU), carboxylated graphite oxide (GO_COOH) and the ibuprofen/carboxylated graphite oxide composite (IBU/GO_COOH); (**c**) ibuprofen (IBU), sulfonated graphite oxide (GO_OSO_3H) and the ibuprofen/sulfonated graphite oxide composite (IBU/GO_OSO_3H).

The thermogravimetric and differential thermal analyses performed on the ibuprofen/graphite oxide composite (IBU/GO) are compared to those of GO in Figure 4. The TGA curve of GO (Figure 4a) presents a 14% weight loss up to 140 °C, indicative of the desorption of water molecules that had adsorbed on GO during exposure to ambient air. The DTA curve shows an exothermic peak at 240 °C caused by the removal of functional groups (hydroxyl, carboxyl and epoxy), which is followed by a weight loss of 26 wt.%. A second exothermic peak is observed at 500 °C due to the combustion of the carbon network, which is followed by the total weight loss of the sample (~60 wt.%) [35]. In the case of

IBU/GO (Figure 4b), up to 76 °C a weight loss of 10% is observed, which corresponds to the loss of absorbed water, while the mass loss of ~19.8% in the temperature range between 76 and 181 °C corresponds to the removal of ibuprofen. The DTA curve presents two exothermic peaks; the first one at 237 °C corresponds to the removal of oxygen groups of graphite oxide and is followed by a mass loss of ~19.7%. Above 580 °C, the decomposition of the graphitic lattice starts, finally accounting for a weight loss of 49.5%.

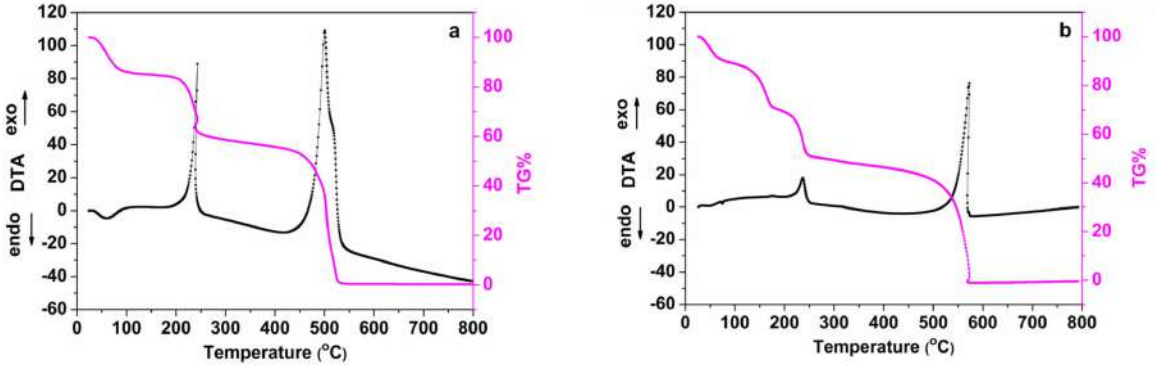

Figure 4. Thermogravimetric analysis (TGA) and differential thermal analysis (DTA) of (**a**) graphite oxide (GO), (**b**) the ibuprofen/graphite oxide composite (IBU/GO).

In Figure 5a, the XRD patterns of ibuprofen (IBU), graphite oxide (GO) and the ibuprofen/graphite oxide composite (IBU/GO) are presented. Pure ibuprofen is characterized [29] by reflections at 2θ = 6.13°, 16.6° and 20.27°, while GO exhibits the principal 001 reflection at 11.26°, corresponding to a basal spacing of 7.85 Å. The diverse oxygen-containing functional groups in the interlayer space of GO adsorb water from the atmosphere, and the basal spacing varies between 6.1 and 11 Å depending on the amount of water adsorbed [36]. In the case of the composites, all the characteristic IBU peaks appear in the pattern, confirming that the ibuprofen has been successfully incorporated in GO. Moreover, the peaks at 2θ = 9.14° and 11.6° allow for conclusions about the way in which the ibuprofen is inserted between the GO sheets. In fact, the peak at 2θ = 9.1° corresponds to the 001 peak, which is indicative of the intercalation of ibuprofen between the graphene sheets. The interlayer space increases to 9.68 Å, and from the size of ibuprofen (approximately 1.0 nm in length, 0.5 nm in width and 0.4 nm in height) [37], we can conclude that the molecules are oriented parallel to the graphene sheets (in agreement with computational results, see below). The fact that the 001 reflection peak of pure GO is present also for the final material leads us to conclude that graphite oxide is not fully intercalated with ibuprofen but that large enough domains of unperturbed GO are present to give rise to diffraction.

In Figure 5b, the XRD patterns of GO_COOH and IBU are compared with that of IBU/GO_COOH. As for GO, ibuprofen reflections located at 2θ = 6.1°, 16.6°, and 20.3° [29] are also distinguishable in the pattern of IBU/GO_COOH and confirm the successful intercalation of the drug in the matrix. The basal spacing of GO_COOH as deduced from the reflection at 2θ = 10.7° is 8.23 Å [28], while for IBU/GO_COOH the basal spacing deduced from the peak 2θ = 11.3° is 7.85 Å, i.e., smaller than for the matrix alone. This leads to the conclusion that ibuprofen must be attached to the surface and to the edges of the GO sheets, creating tensions to the edges, which cause a minor reduction in the interlayer space of the composite.

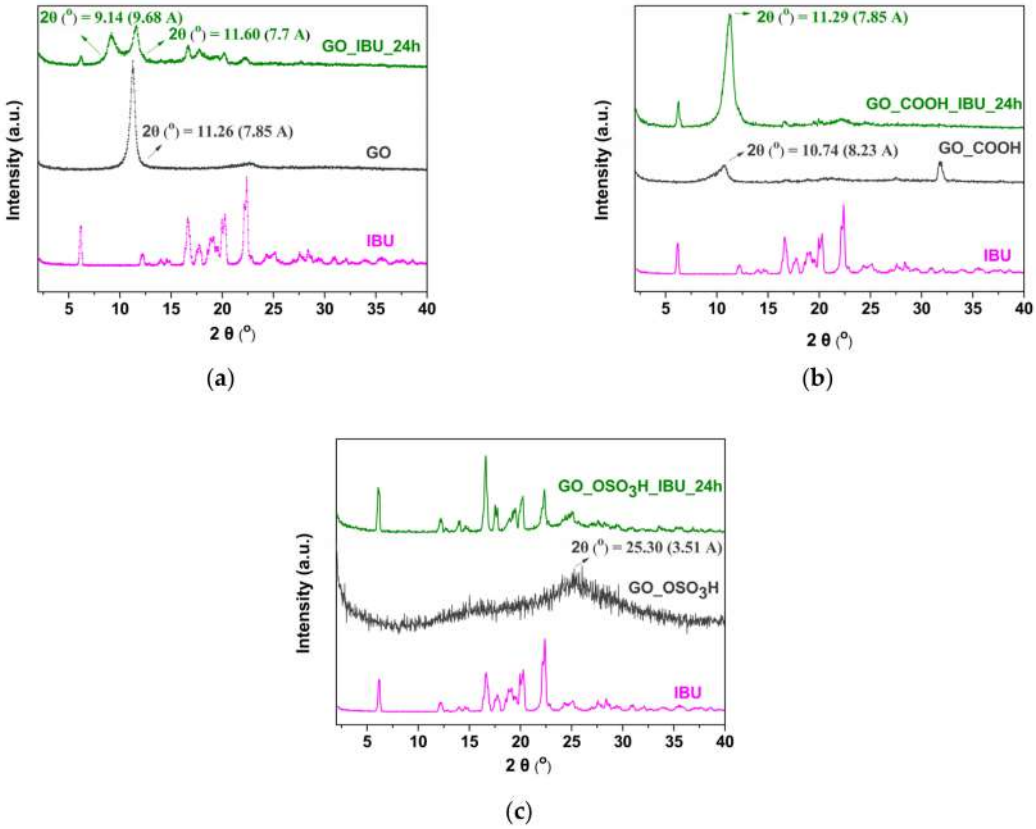

Figure 5. XRD pattern of (**a**) ibuprofen (IBU), graphite oxide (GO) and the ibuprofen/graphite oxide composite (IBU/GO); (**b**) ibuprofen (IBU), carboxylated graphite oxide (GO_COOH) and the ibuprofen/carboxylated graphite oxide composite (IBU/GO_COOH); (**c**) ibuprofen (IBU), sulfonated graphite oxide (GO_OSO_3H) and the ibuprofen/sulfonated graphite oxide composite (IBU/GO_OSO_3H).

The diffraction patterns of IBU, GO_OSO_3H and IBU/GO_OSO_3H are presented in Figure 5c. In the pattern of sulfonated graphite oxide, the 002 reflection peak at $2\theta = 25.0°$ corresponds to a basal spacing of 3.51 Å. The presence of this peak implies that after sulfonation, the exfoliated sheets restack through π–π interactions [27]. Again, the peaks characteristic of ibuprofen are distinguished in the composite. Due to the specific structure of GO after the sulfonation reaction, interaction with ibuprofen causes its total exfoliation, as deduced from the absence of the characteristic 001 and 002 peaks. Summarizing XRD patterns from Figure 5, we conclude that IBU released into simulated gastric and intestinal juice comes from the surface and interlayer space for GO_IBU, while for IBU/GO_COOH the release comes mainly from the surface but also the intercalated edges of GO_COOH. Finally, for the GO_OSO_3H, the release of IBU comes from the surface of exfoliated GO_OSO_3H.

Detailed AFM images of flakes of the different carbon nanostructures are shown in Figure 6. The average thickness of the flakes was 1.5–2.5 nm as derived from the topographic height profile (section analysis). The thickness of the un-modified IBU/GO part in Figure 6a was 2.26 nm and the part of GO modified with ibuprofen had a thickness of 7.93 nm. Similarly, in the AFM image (Figure 6b) of IBU/GO_COOH, the unmodified and the IBU-modified part differ in thickness by 9.5 nm, while for IBU/GO_OSO_3H, respectively, the carbon nanosheets of graphene oxide and the their topographical height are depicted, which indicates the successful modification with -COOH and $-OSO_3H$ groups alongside ibuprofen (Figure 6c).

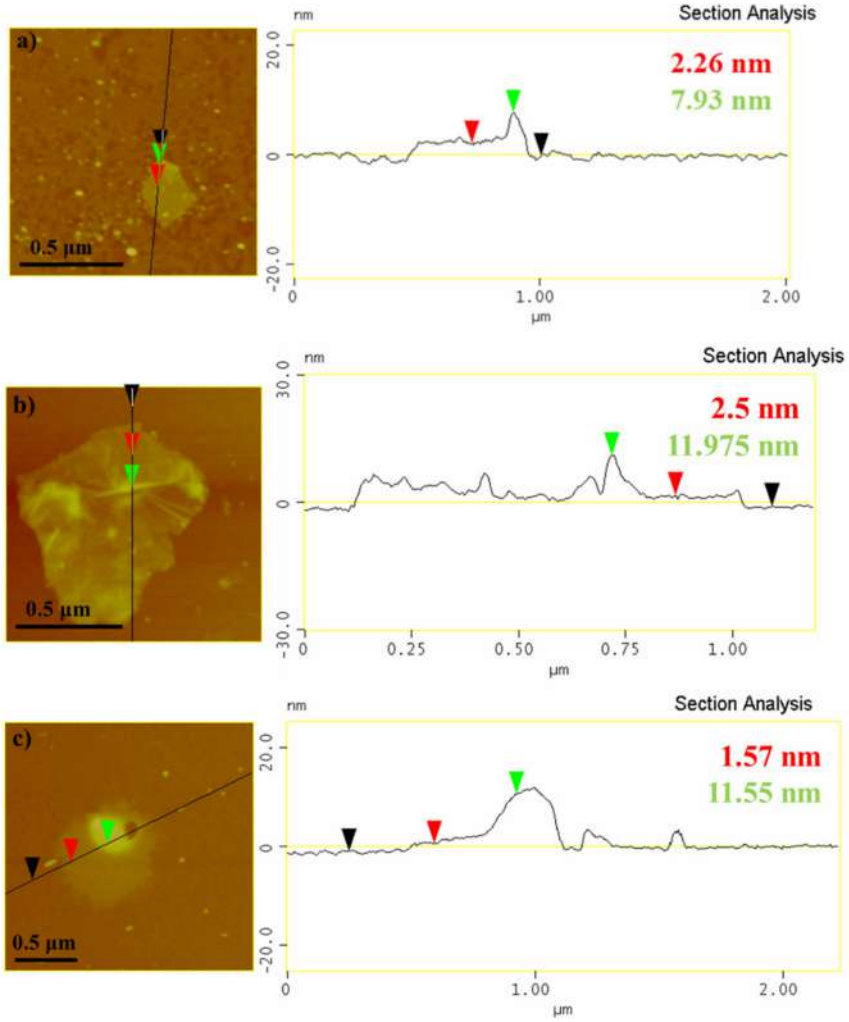

Figure 6. AFM cross section analysis of the composites (**a**) ibuprofen/graphite oxide (IBU/GO), (**b**) ibuprofen/carboxylated graphite oxide (IBU/GO_COOH), (**c**) ibuprofen/sulfonated graphite oxide (IBU/GO_OSO_3H).

3.2. Theoretical Calculations

The optimized ibuprofen−GO structures are shown in Figures 7–9. The cluster model energies of the GO systems were found to be in close agreement with our experimental results.

3.3. In Vitro Drug Release of Ibuprofen

The amount of IBU loaded in the three graphene-based matrices was estimated by subtracting the IBU concentration in the supernatant of the GO hybrids (measured by UV–Vis spectroscopy) from the initial concentration of the drug. The IBU determined in this fashion amounted to 0.810 mmol/g for IBU/GO, 0.791 mmol/g for IBU/GO_OSO_3H and 0.743 mmol/g for IBU/GO_COOH.

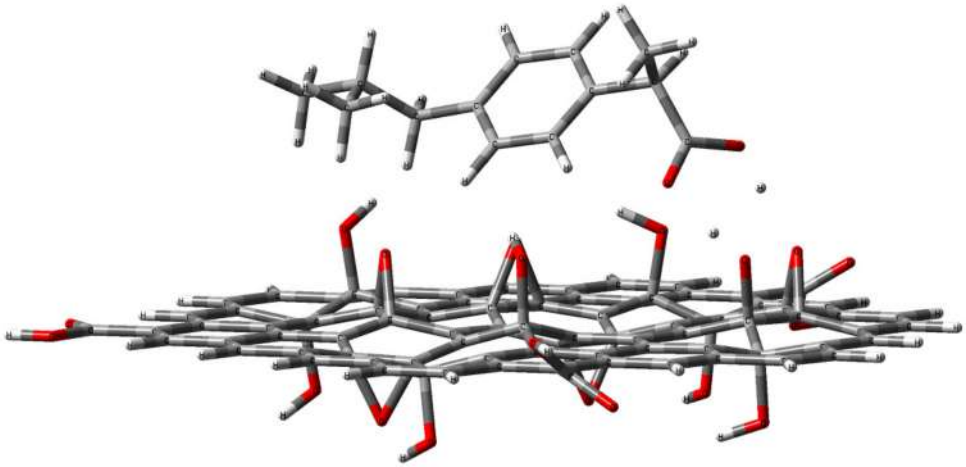

Figure 7. Optimized geometry (position and orientation) calculated at the B3LYP/3-21G* level of theory for the adsorbed ibuprofen molecule (side view) on the single-layer hydroxylated graphene oxide modeled by the depicted cluster ($C_{80}H_{30}O_{18}$) GO, which contains three anchored COOH groups on its edge and eight hydroxyl and six epoxy groups divided between the top and bottom surfaces. DE = −36.5 kcal/mol.

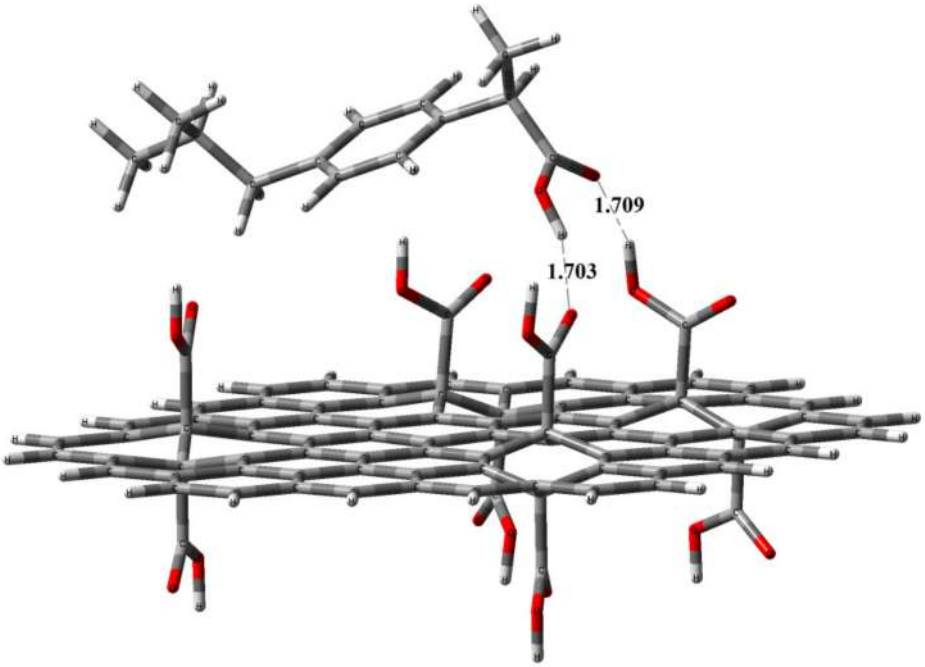

Figure 8. Optimized geometry (position and orientation) calculated at the B3LYP/3-21G* level of theory for the adsorbed ibuprofen molecule (side view) on the single-layer carboxylated graphene oxide modeled by the depicted cluster ($C_{80}H_{30}O_{16}$) GO_COOH, which contains eight anchored COOH groups divided between the top and bottom surfaces. DE = −32.4 kcal/mol.

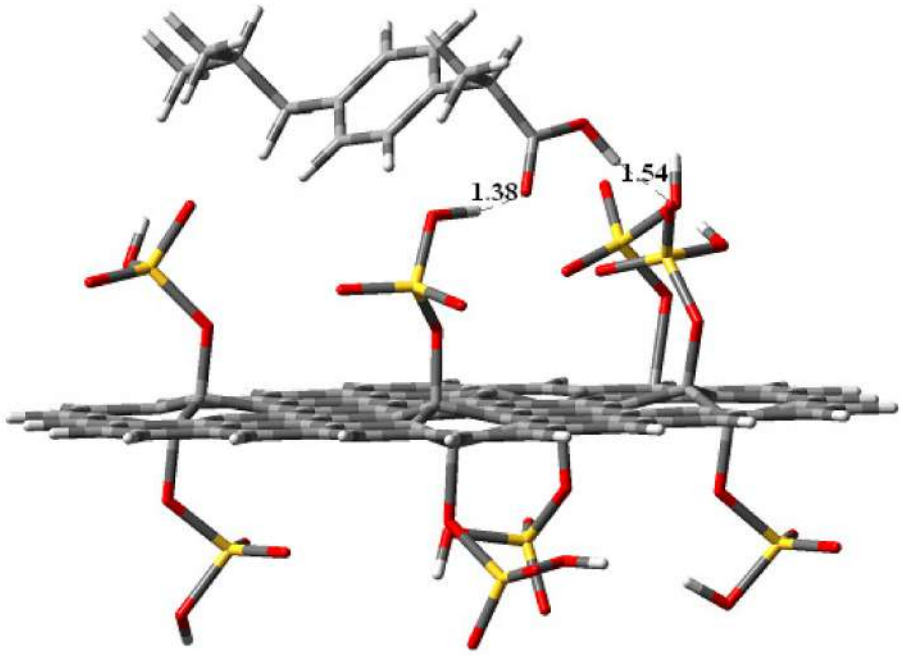

Figure 9. Optimized geometry (position and orientation) calculated at the B3LYP/3-21G* level of theory for the adsorbed ibuprofen molecule (side view) on the single-layer sulfonated graphene oxide modeled by the depicted cluster ($C_{80}H_{30}O_{32}S_8$) GO_OSO_3H, which contains eight anchored OSO_3H groups divided between the top and bottom surfaces. DE = −30.8 kcal/mol.

The loaded matrices were brought in contact with simulated gastric fluid, and the release of ibuprofen was monitored as described in the Experimental Details. Figure 10 shows the release profiles of IBU from IBU/GO, IBU/GO_COOH and IBU/GO_OSO_3H in gastric fluid at 37 °C. The release of ibuprofen in gastric fluid was relatively low and occurred rather slowly, i.e., after 24 h of incubation, 12.0% of the stored ibuprofen was released from 22.9% from IBU/GO_COOH and IBU/GO, and 19.5% from IBU/GO_OSO_3H, in agreement with theoretical calculations. When the same types of experiments were performed with simulated intestinal fluid, as also shown in Figure 10, the release first happened rapidly and then reached a plateau. Moreover, the amount of ibuprofen released was much larger than in the simulated gastric fluid. Specifically, for IBU/GO, a maximum release of ~43.0% of ibuprofen was reached in 200 min; for IBU/GO_COOH, a release of ~45.9% was reached in 150 min; and for IBU/GO_OSO_3H, a release of ~43.4% was reached in 60 min. The more gradual release of ibuprofen in gastric fluid as compared to that in intestinal fluid holds potential for eliminating the stomach-related side effects of ibuprofen. The ibuprofen release from the three types of carbon nanomaterials that were used in this project (GO, GO_COOH and GO_OSO_3H) performed much better than from montmorillonite, which was tested as a drug carrier in a previous study [29]. The statistical error bar for all calculations was estimated at approximately 2%. For every release spot we tested, 3 samples were run in triplicate.

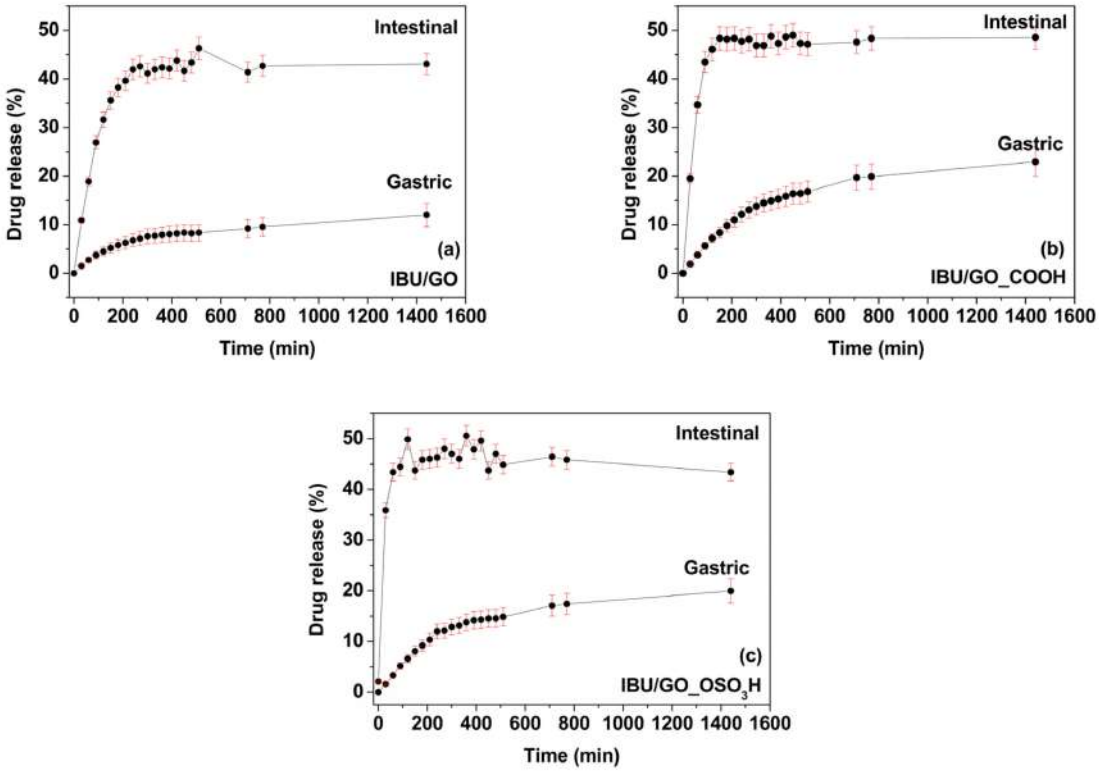

Figure 10. Release profiles of (**a**) IBU/GO, (**b**) IBU/GO_COOH and (**c**) IBU/GO_OSO_3H in simulated gastric and intestinal fluid.

4. Conclusions

In this study, graphite oxide and two of its derivatives, sulfonated graphite oxide and carboxylated graphite oxide, were prepared, and their efficacy as drug delivery systems for ibuprofen was investigated. For all three carriers, the release of ibuprofen occurred more gradually in gastric fluid than in intestinal fluid. The more "controllable" release in gastric fluid holds potential for eliminating or mitigating the very common gastrointestinal side effects of heartburn and abdominal pain observed after ibuprofen administration to patients.

Author Contributions: Conceptualization, P.Z., D.G. and P.R.; methodology, P.Z., K.S., D.K.P., E.D., H.S., D.G. and P.R.; validation, P.Z., K.S., D.K.P., E.D., H.S., D.G. and P.R.; formal analysis, P.Z., K.S., G.A. and D.K.P.; investigation, P.Z., K.S., D.K.P., G.A., E.D., H.S., D.G. and P.R.; writing—original draft preparation, P.Z., K.S., G.A. and D.K.P.; writing—review and editing, P.Z., K.S., D.K.P., E.D., H.S., D.G. and P.R.; visualization, P.Z., K.S., D.K.P., E.D., H.S., D.G. and P.R.; supervision, P.Z., D.G. and P.R. All authors have read and agreed to the published version of the manuscript.

Funding: This research received no external funding.

Institutional Review Board Statement: Not applicable.

Informed Consent Statement: Not applicable.

Data Availability Statement: Not applicable.

Acknowledgments: P.Z. and K.S. acknowledge the Ubbo Emmius Program for PhD fellowships.

Conflicts of Interest: The authors declare no conflict of interest.

References

1. Williams, H.D.; Trevaskis, N.L.; Charman, S.A.; Shanker, R.M.; Charman, W.N.; Pouton, C.W.; Porter, C.J.H. Strategies to Address Low Drug Solubility in Discovery and Development. *Pharmacol. Rev.* **2013**, *65*, 315–499. [CrossRef] [PubMed]
2. Bonthagarala, B.; Lakshmi Sai, P.D.L.; Venkata, S.K.; Rao, B.N.; Dasari, V. Enhancement of dissolution rate of Clofibrate BCS Class II drug by using liquisolid compact technology. *Int. J. Biomed. Adv. Res.* **2015**, *6*, 288. [CrossRef]
3. Tiwari, G.; Tiwari, R.; Sriwastawa, B.; Bhati, L.; Pandey, S.; Pandey, P.; Bannerjee, S.K. Drug delivery systems: An updated review. *Int. J. Pharm. Investig.* **2012**, *2*, 2–11. [CrossRef]
4. Lim, D.-J.; Sim, M.; Oh, L.; Lim, K.; Park, H. Carbon-based drug delivery carriers for cancer therapy. *Arch. Pharmacal Res.* **2014**, *37*, 43–52. [CrossRef] [PubMed]
5. Senapati, S.; Mahanta, A.K.; Kumar, S.; Maiti, P. Controlled drug delivery vehicles for cancer treatment and their performance. *Signal Transduct. Target Ther.* **2018**, *3*, 7. [CrossRef] [PubMed]
6. Rauti, R.; Musto, M.; Bosi, S.; Prato, M.; Ballerini, L. Properties and behavior of carbon nanomaterials when interfacing neuronal cells: How far have we come? *Carbon* **2019**, *143*, 430–446. [CrossRef]
7. Mohajeri, M.; Behnam, B.; Sahebkar, A. Biomedical applications of carbon nanomaterials: Drug and gene delivery potentials. *J. Cell. Physiol.* **2018**, *234*, 298–319. [CrossRef]
8. Liu, W.; Speranza, G. Functionalization of Carbon Nanomaterials for Biomedical Applications. *C* **2019**, *5*, 72. [CrossRef]
9. Hong, J.; Shah, N.J.; Drake, A.C.; DeMuth, P.C.; Lee, J.B.; Chen, J.; Hammond, P.T. Graphene Multilayers as Gates for Multi-Week Sequential Release of Proteins from Surfaces. *ACS Nano* **2012**, *6*, 81–88. [CrossRef]
10. Oliveira, A.M.L.; Machado, M.; Silva, G.A.; Bitoque, D.B.; Tavares Ferreira, J.; Pinto, L.A.; Ferreira, Q. Graphene Oxide Thin Films with Drug Delivery Function. *Nanomaterials* **2022**, *12*, 1149. [CrossRef] [PubMed]
11. Machado, M.; Silva, G.A.; Bitoque, D.B.; Ferreira, J.; Pinto, L.A.; Morgado, J.; Ferreira, Q. Self-Assembled Multilayer Films for Time-Controlled Ocular Drug Delivery. *ACS Appl. Bio Mater.* **2019**, *2*, 4173–4180. [CrossRef] [PubMed]
12. Campbell, E.; Hasan, M.T.; Pho, C.; Callaghan, K.; Akkaraju, G.R.; Naumov, A.V. Graphene Oxide as a Multifunctional Platform for Intracellular Delivery, Imaging, and Cancer Sensing. *Sci. Rep.* **2019**, *9*, 416. [CrossRef]
13. Chen, L.; Batchelor-McAuley, C.; Rasche, B.; Johnston, C.; Hindle, N.; Compton, R.G. Surface area measurements of graphene and graphene oxide samples: Dopamine adsorption as a complement or alternative to methylene blue? *Appl. Mater. Today* **2020**, *18*, 100506. [CrossRef]
14. Liu, J.; Cui, L.; Losic, D. Graphene and graphene oxide as new nanocarriers for drug delivery applications. *Acta Biomater.* **2013**, *9*, 9243–9257. [CrossRef]
15. Mojgan, N.; Fahimeh, C.; Mohammad, R. Graphene as multifunctional delivery platform in cancer therapy. *J. Biomed. Mater. Res. Part A* **2017**, *105*, 2355–2367. [CrossRef]
16. Zhang, B.; Yan, Y.; Shen, Q.; Ma, D.; Huang, L.; Cai, X.; Tan, S. A colon targeted drug delivery system based on alginate modificated graphene oxide for colorectal liver metastasis. *Mater. Sci. Eng. C* **2017**, *79*, 185–190. [CrossRef]
17. Mo, R.; Jiang, T.; Sun, W.; Gu, Z. ATP-responsive DNA-graphene hybrid nanoaggregates for anticancer drug delivery. *Biomaterials* **2015**, *50*, 67–74. [CrossRef]
18. Usman, M.; Hussein, M.; Kura, A.; Fakurazi, S.; Masarudin, M.; Ahmad Saad, F. Graphene Oxide as a Nanocarrier for a Theranostics Delivery System of Protocatechuic Acid and Gadolinium/Gold Nanoparticles. *Molecules* **2018**, *23*, 500. [CrossRef]
19. Parveen, S.; Misra, R.; Sahoo, S.K. Nanoparticles: A boon to drug delivery, therapeutics, diagnostics and imaging. *Nanomed. Nanotechnol. Biol. Med.* **2012**, *8*, 147–166. [CrossRef]
20. Dembereldorj, U.; Kim, M.; Kim, S.; Ganbold, E.-O.; Lee, S.Y.; Joo, S.-W. A spatiotemporal anticancer drug release platform of PEGylated graphene oxide triggered by glutathione in vitro and in vivo. *J. Mater. Chem.* **2012**, *22*, 23845–23851. [CrossRef]
21. Tian, B.; Wang, C.; Zhang, S.; Feng, L.; Liu, Z. Photothermally Enhanced Photodynamic Therapy Delivered by Nano-Graphene Oxide. *ACS Nano* **2011**, *5*, 7000–7009. [CrossRef]
22. Yang, Y.; Ying-Ming, Z.; Yong, C.; Di, Z.; Jia-Tong, C.; Yu, L. Construction of a Graphene Oxide Based Noncovalent Multiple Nanosupramolecular Assembly as a Scaffold for Drug Delivery. *Chem. Eur. J.* **2012**, *18*, 4208–4215. [CrossRef]
23. Wojtoniszak, M.; Urbas, K.; Perużyńska, M.; Kurzawski, M.; Droździk, M.; Mijowska, E. Covalent conjugation of graphene oxide with methotrexate and its antitumor activity. *Chem. Phys. Lett.* **2013**, *568–569*, 151–156. [CrossRef]
24. Hu, H.; Tang, C.; Yin, C. Folate conjugated trimethyl chitosan/graphene oxide nanocomplexes as potential carriers for drug and gene delivery. *Mater. Lett.* **2014**, *125*, 82–85. [CrossRef]
25. Dong, H.; Dai, W.; Ju, H.; Lu, H.; Wang, S.; Xu, L.; Zhou, S.-F.; Zhang, Y.; Zhang, X. Multifunctional Poly(l-lactide)–Polyethylene Glycol-Grafted Graphene Quantum Dots for Intracellular MicroRNA Imaging and Combined Specific-Gene-Targeting Agents Delivery for Improved Therapeutics. *ACS Appl. Mater. Interfaces* **2015**, *7*, 11015–11023. [CrossRef] [PubMed]
26. Spyrou, K.; Calvaresi, M.; Diamanti, E.K.; Tsoufis, T.; Gournis, D.; Rudolf, P.; Zerbetto, F. Graphite Oxide and Aromatic Amines: Size Matters. *Adv. Funct. Mater.* **2015**, *25*, 263–269. [CrossRef]
27. Liu, J.; Xue, Y.; Dai, L. Sulfated Graphene Oxide as a Hole-Extraction Layer in High-Performance Polymer Solar Cells. *J. Phys. Chem. Lett.* **2012**, *3*, 1928–1933. [CrossRef]
28. Ciobotaru, C.C.; Damian, C.M.; Matei, E.; Iovu, H. Covalent Functionalization of Graphene Oxide with Cisplatin. *Mater. Plast.* **2014**, *51*, 75–80.

29. Zheng, J.P.; Luan, L.; Wang, H.Y.; Xi, L.F.; Yao, K.D. Study on ibuprofen/montmorillonite intercalation composites as drug release system. *Appl. Clay Sci.* **2007**, *36*, 297–301. [CrossRef]
30. Lee, S.W.; Condrate, R.A. The infrared and Raman spectra of ZrO_2-SiO_2 glasses prepared by a sol-gel process. *J. Mater. Sci.* **1988**, *23*, 2951–2959. [CrossRef]
31. Becke, A.D. Density-functional thermochemistry. III. The role of exact exchange. *J. Chem. Phys.* **1993**, *98*, 5648–5652. [CrossRef]
32. Frisch, M.J.; Trucks, G.W.; Schlegel, H.B.; Scuseria, G.E.; Robb, M.A.; Cheeseman, J.R.; Scalmani, G.; Barone, V.; Mennucci, B.; Petersson, G.A.; et al. *Gaussian 09*; Revision B.01; Gaussian, Inc.: Wallingford, CT, USA, 2009.
33. Dobbs, K.D.; Hehre, W.J. Molecular orbital theory of the properties of inorganic and organometallic compounds 4. Extended basis sets for third-and fourth-row, main-group elements. *J. Comput. Chem.* **1986**, *7*, 359–378. [CrossRef]
34. Namur, J.; Wassef, M.; Pelage, J.P.; Lewis, A.; Manfait, M.; Laurent, A. Infrared microspectroscopy analysis of Ibuprofen release from drug eluting beads in uterine tissue. *J. Control. Release* **2009**, *135*, 198–202. [CrossRef]
35. Song, J.; Wang, X.; Chang, C.-T. Preparation and Characterization of Graphene Oxide. *J. Nanomater.* **2014**, *2014*, 276143. [CrossRef]
36. Dékány, I.; Krüger-Grasser, R.; Weiss, A. Selective liquid sorption properties of hydrophobized graphite oxide nanostructures. *Colloid Polym. Sci.* **1998**, *276*, 570–576. [CrossRef]
37. Mestre, A.S.; Pires, J.; Nogueira, J.M.F.; Carvalho, A.P. Activated carbons for the adsorption of ibuprofen. *Carbon* **2007**, *45*, 1979–1988. [CrossRef]